Supporting Information

Natarajan et al. 10.1073/pnas.1304988111

SI Methods

RNA Isolation and Microarray. Total RNA was isolated from B16 cells or whole epidermal cells from punch biopsies after separation of dermis using Dispase II as indicated earlier (1).Whole-genome microarray was carried out using Illumina WG-6 array, and preliminary data normalization and analysis carried out using Beadstudio software using manufacturer's instructions.

Western Blot Analysis, Immunochemical Method, and Microscopy. Rabbit α-hTRP2 antibody [against dopachrome tautomerase (DCT); 1:1,000; Abcam], mouse α–h-tyrosinase (1:500; Dako), rabbit α–h-pSTAT1(Y701) (1:1,000; Cell Signaling Technology), mouse α–h-microphthalmia-associated transcription factor (α-hMITF; C5 clone; gift from David E. Fisher, Massachusetts General Hospital, Boston), and HRP α-tubulin (1:2,000; Cell Signaling Technology) were used for Western blot analysis. For tracking melanosomes, melanocytes were grown in LabTek chamber coverglass, fixed, permeabilized, stained with HMB45 followed by secondary Alexa fluor 488, and counterstained with DAPI. The cells were imaged and analyzed with a Ziess LSM 510 Meta confocal microscope. For transmission EM studies, ultrathin sections (80 nm) were cut on an RMC Ultramicrotome, placed on copper grids, stained with uranyl acetate and lead citrate, and examined on a JEM 2100F transmission electron microscope.

Constructs and Transfections. The Dct 3,745-bp promoter (−3,300 to +445 bp from Dct transcription start site) was amplified by PCR and cloned upstream of a luciferase cassette in SacI/XhoI sites of pGL4.23 (Promega). Deletions in the construct were made by site-directed mutagenesis (Stratagene) according to the manufacturer's protocol. Mouse IFN regulatory factor-1 (Irf1)/pcDNA construct was a gift from Nicole Clarke (The University of Nottingham, Nottingham, UK). Transfections were set up at day 3 of low-density cycle with a 6:1 ratio of Cellfectin (Invitrogen) to DNA. Renilla luciferase driven by CMV promoter was cotransfected for normalizations. Posttransfection, low-density media were replaced, and treatments were done; 48 h posttransfection, the cells were lysed with passive lysis buffer (Promega), and luciferase assays were performed according to the manufacturer's protocol (Dual-Luciferase Reporter Assay System; Promega).

siRNA Transfection. Human foreskin-derived melanocytes were plated in antibiotic-free M254 media with supplements at a density of 2×10^5 cells per well of a six-well plate. Transfection was carried out with Cellfectin reagent (Invitrogen) as per the manufacture's protocol. The siRNA concentration used was 100 nM for all siRNAs. Briefly, the cells were incubated with siRNA–cellfectin complexes for 6 h followed by trypsinization of the cells and replating in 24-well plates; 4 h after replating, IFN-γ was added at a concentration of 100 U/mL in the required wells, and 48 h after IFN-γ addition, the cells were harvested for RNA isolation.

Cell Cycle Analysis by Propidium Iodide Staining. Primary human cells were treated with 100 U/mL IFN-γ for 5 d, and the cells were trypsinized and washed one time in 5–10 mL 1× PBS. The cells were resuspended in 1 mL paraformaldehyde fixation solution and incubated on ice for 1 h. Paraformaldehyde was washed using 5 mL 1× PBS, and the cell pellet was resuspended in 0.5 mL 1× PBS; 4.5 mL ice cold 70% ethanol were added dropwise over 30 s to 1 min, and the cells were incubated at 4 °C overnight. The cells were then resuspended in 0.5 mL Propidium Iodide (5 mg/mL) staining solution, incubated for 30 min at 37 °C, and analyzed by flow cytometry. The cells were gated based on the DNA content, and the percentages of cells in each stage of the cell cycle were analyzed based on the nuclear content.

Bead Assay for Detection of Protein Bound to Biotinylated *Dct* Promoter. Biotinylated 3.7-kb Dct promoter was immobilized with avidin-agarose beads (Sigma) followed by incubation with IFN-γ–treated B16 cells for 4 h at 4 °C on a rocker. The supernatant was discarded, and the DNA-bead–bound proteins were washed three times with buffer (10 mM Hepes, 10 mM KCl, 0.1 M EDTA, 0.1 M EGTA, 1× protease inhibitor mixture). The bound proteins were eluted by heating the samples with SDS sample dye at 100 °C for 5 min and loaded onto SDS/PAGE gel followed by Western blot analysis with mouse IRF1 antibody (M-20; Santa Cruz). Nonbiotinylated 3.7-kb Dct promoter was used as control in this assay.

Quantitation of Pigmentaion by Image Analysis. Images of $IFNG^{+/+}$ and $IFNG^{-/-}$ mice were captured using the Nikon camera under similar lighting conditions. For quantifications, 22 measurements were made for each mouse across each earlobe, and mean gray values were calculated (ImageJ).

SI Text

Detection of IFN-γ in the Oscillator Model.

i) Measurement of IFN-γ by ELISA in culture supernatants over the course of pigmentation and depigmentation was performed. As low as 0.01 U/mL recombinant mouse IFN-γ could be detected. There were no detectable levels of IFN-γ in the culture supernatants throughout the cycle.

ii) Real-time PCR detection of IFN-γ transcripts was carried out. IFN-γ mRNA could be detected from splenocyte cells that served as positive control. However, IFN-γ transcripts could not be detected at all phases of the oscillator.

iii) Addition of blocking antibody to IFN-γ during the course of depigmentation did not alter the depigmentation kinetics or the downstream gene expression changes.

Based on all these observations, we conclude that B16 cells do not actively secrete IFN-γ, and the activation of IFN-γ signaling is most likely to occur independent of the known cognate ligand. Several studies in the literature have reported such ligand-independent signaling activation (2, 3).

Future studies should examine this pathway in the laboratory. The key finding based on transcriptome signatures that resulted in identification of IFN-γ as an important mediator of melanogenesis holds true, and the significance of this finding is supported by experiments in multiple model systems. Other than B16 cells, we have performed these studies in primary melanocytes obtained from different subjects. The density-dependent model does not function in primary melanocytes, because cell–cell contact is important for culturing these cells. Moreover, proliferation and melanogenesis are tightly coupled in primary cells through MITF (4).

1. Natarajan VT, et al. (2010) Transcriptional upregulation of Nrf2-dependent phase II detoxification genes in the involved epidermis of vitiligo vulgaris. *J Invest Dermatol* 130(12):2781–2789.
2. Costa-Pereira AP, et al. (2002) Mutational switch of an IL-6 response to an interferon-gamma-like response. *Proc Natl Acad Sci USA* 99(12):8043–8047.
3. Gao B (2012) Wnt regulation of planar cell polarity (PCP). *Curr Top Dev Biol* 101: 263–295.
4. Nishimura EK, et al. (2010) Key roles for transforming growth factor beta in melanocyte stem cell maintenance. *Cell Stem Cell* 6(2):130–140.

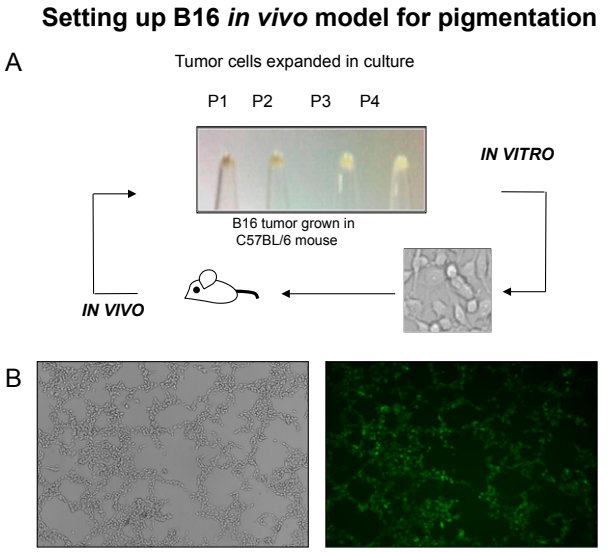

Fig. S1. Setting up the B16 in vivo model for pigmentation. (*A*) B16 cells were grown as tumor in C57BL/6 mice. The tumor was dispersed and grown in vitro as an adherent culture. Cells were harvested, and pellets from days 4 [passage 1 (P1)], 8 (P2), 12 (P3), and 16 (P4) were imaged. Cells progressively depigmented and were completely devoid of melanin by P4. When these cells were injected back into the animal and grown as tumor, the cells regained pigmentation. (*B*) B16 melanoma cells obtained from a tumor using a B16 clone stably expressing GFP (TNV2). (*Left*) Phase contrast. (*Right*) GFP.

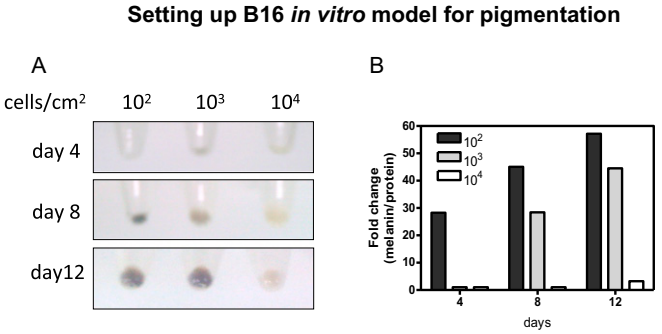

Fig. S2. Setting up the B16 in vitro model for pigmentation. (*A*) B16 cells were plated at the indicated cell density for 4, 8, and 12 d. Cells were harvested, and pellets were imaged. (*B*) Melanin and protein estimations were carried out from the cells, and the ratio of the two is indicated.

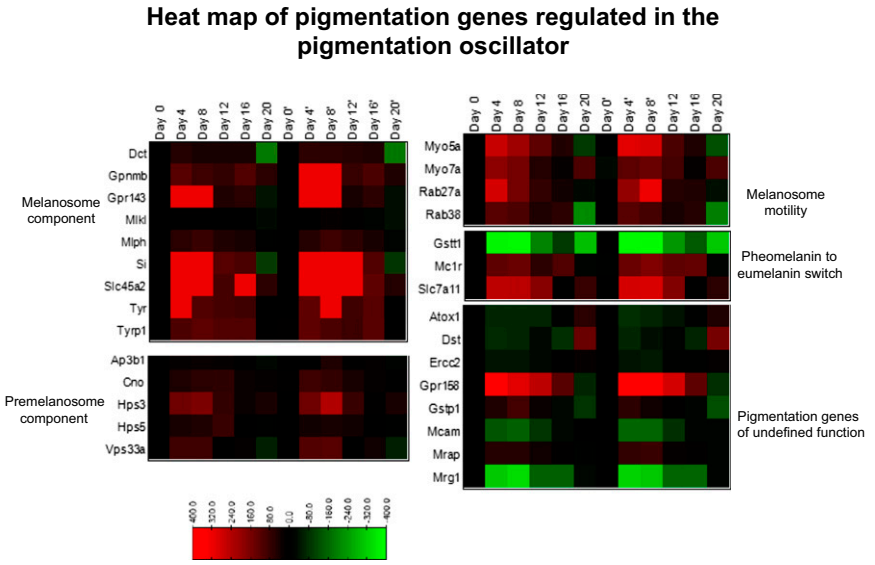

Fig. S3. Heat map of pigmentation genes regulated in the pigmentation oscillator. Genes involved in various melanosome-related processes, such as melanosomal component, premelanosomal component, melanosomal motility, and pheomelanin to eumelanin switch, were chosen, and the relative expression level of these genes in the two cycles with respect to day 0 is represented as a heat map.

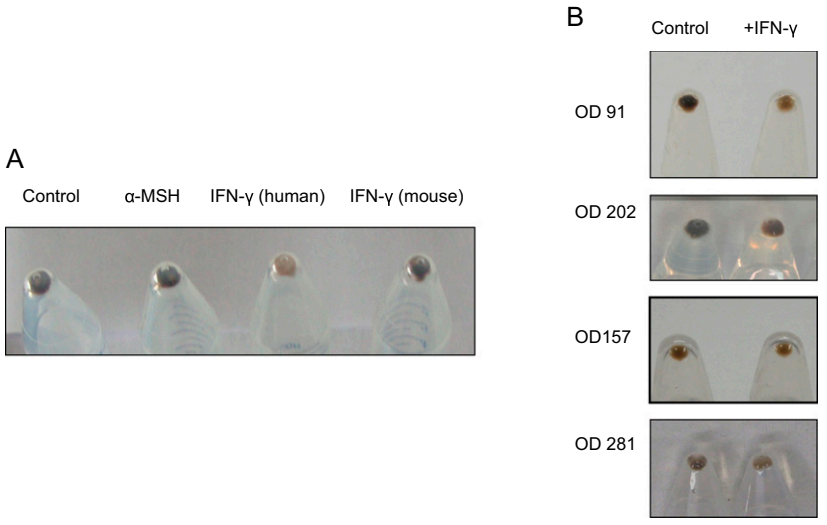

Fig. S4. Primary human melanocytes are hypopigmented with human IFN-γ treatment. (*A*) Primary human melanocytes were treated with 600 nM α-melanocyte stimulating hormone (α-MSH; known propigmenting agent), human IFN-γ (100 U/mL), or mouse IFN-γ (100 U/mL) for 7 d, after which time the cell pellets were observed. Only human IFN-γ caused visible hypopigmentation. (*B*) Four independent primary melanocyte cultures obtained from neonatal foreskin show visible hypopigmentation with IFN-γ treatment.

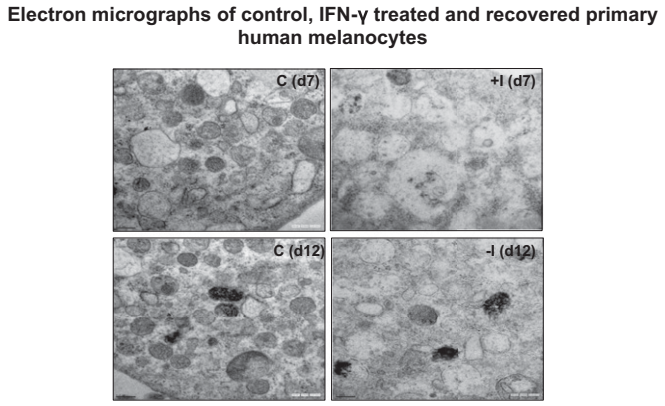

Fig. S5. Electron micrographs of control (C) and IFN-γ–treated (+I) and recovered (−I) primary human melanocytes. Electron micrographs of primary human melanocytes were either left untreated [C (d7)] or treated with human IFN-γ [100 U/mL; +I(d7)] for 7 d, after which time IFN-γ was withdrawn from the cultures and grown until day 12. C(d12) and −I(d12) represent electron micrographs of control and IFN-γ–recovered cells, respectively. As is clear from the pictures, after withdrawal of IFN-γ, −I(d12) looks similar to control [C(d12)], thus showing the recovery.

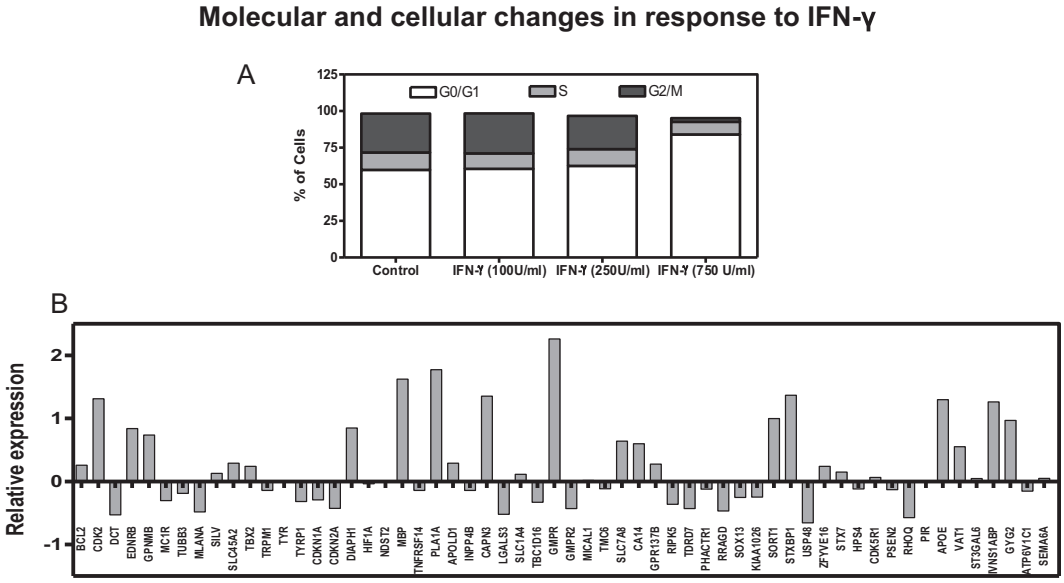

Fig. S6. Molecular and cellular changes in response to IFN-γ. (*A*) Cell cycle analysis of primary human melanocytes treated with IFN-γ for 7 d was carried out using flow cytometry. The percentage of cells in different phases of the cell cycle is represented as a bar chart. (*B*) Expression level of known MITF target genes expressed as log (fold change after IFN-γ treatment) from microarray analysis of IFN-γ–treated melanocytes.

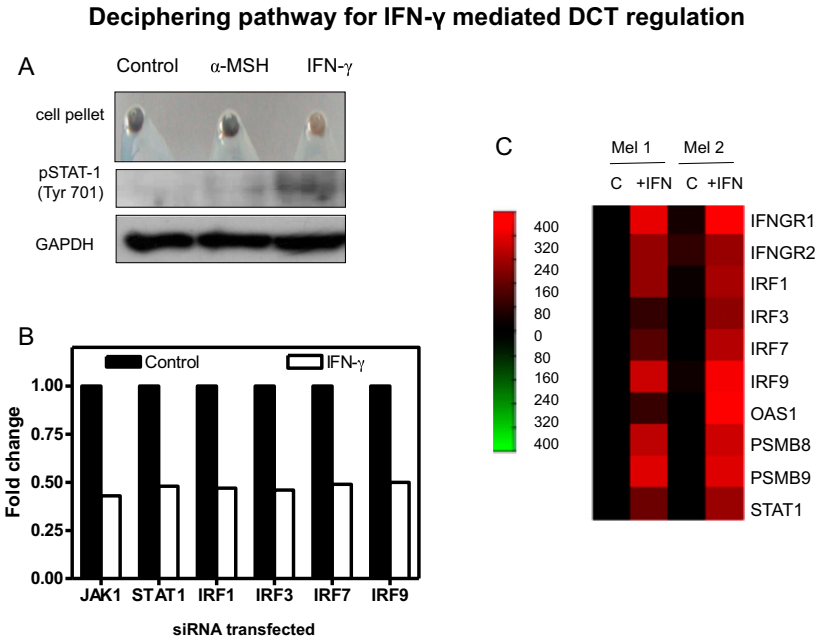

Fig. S7. Deciphering the pathway for IFN-γ–mediated DCT regulation. (*A*) Primary human melanocyte cultures were treated with α-MSH (600 nM) and IFN-γ (100 U/mL), and Western blot analysis was performed with α-pSTAT-1 antibody. GAPDH was used as an equal loading control. (*B*) Primary human melanocytes were transfected with 100 nM concentration of indicated siRNA, and the mRNA levels for the respective genes were quantitated 48 h posttransfection by using real-time PCR. Fold change in the mRNA levels was calculated with respect to the scrambled siRNA–transfected melanocytes. (*C*) Heat map of genes regulated by IFN-γ in two independent melanocyte cultures (Mel 1 and Mel 2). C, Control.

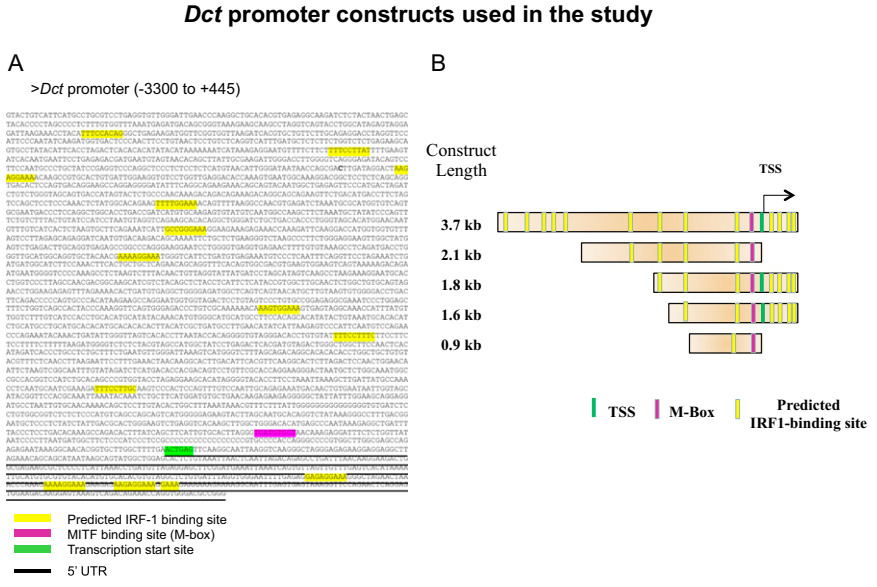

Fig. S8. *Dct* promoter constructs used in the study. (*A*) The full-length 3.7-kb *Dct* promoter with the predicted Irf1 binding sites is highlighted in yellow. (*B*) *Dct* promoter constructs used in our study. M-Box, MITF binding site; TSS, transcription start site.

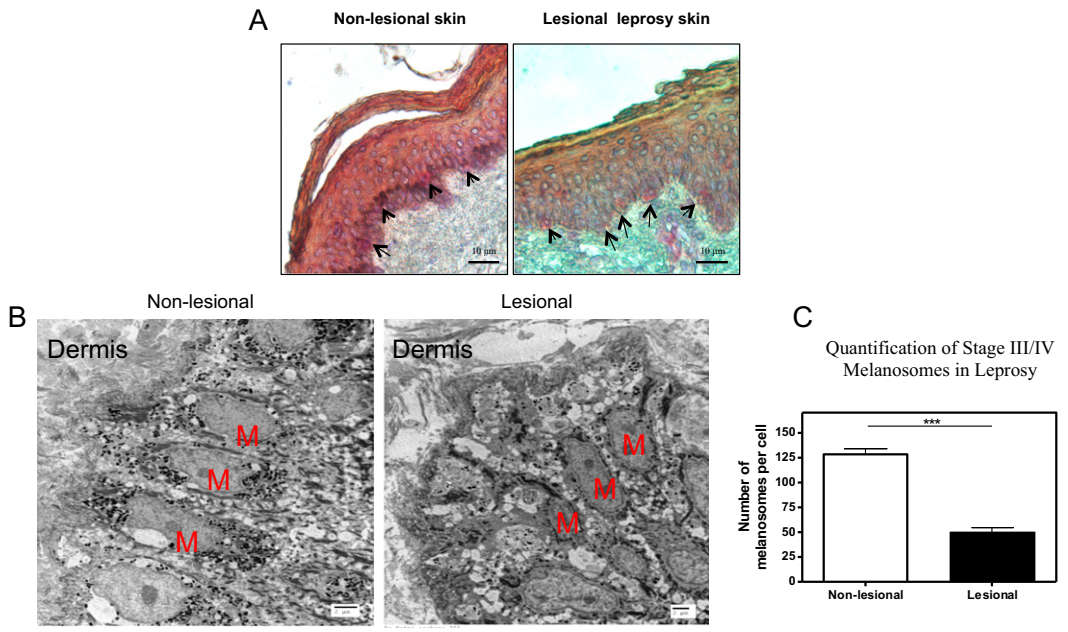

Fig. S9. Analysis of nonlesional and lesional skin from leprosy. (*A*) Immunohistochemical analysis of melanocyte-specific S100 staining in paired nonlesional and lesional leprosy skin. (*B*) Electron micrographs of nonlesional and lesional skin from a leprosy patient showing presence of melanocytes at the epidermal–dermal junction (M). (*C*) Quantitation of stage III and IV melanosomes in 10 melanocytes each from the nonlesional and lesional skin of three leprosy patients. Paired *t* test indicated that the means are significantly different with a *P* value less than 0.001. ***P value < 0.001.

Table S1. List of enriched genes from periodogram analysis of pigmentation oscillator

Serial no.	Fracmaxamp	Illumina identification	Gene name
1	0.949600	ILMN_195590	
2	0.929992	ILMN_209839	Solute carrier family 44, member 2
3	0.909949	ILMN_209574	Cold shock domain containing e1, rna binding
4	0.883781	ILMN_212867	
5	0.871957	ILMN_193770	
6	0.862152	ILMN_211146	
7	0.851477	ILMN_251332	cdna sequence bc006779
8	0.845110	ILMN_211043	cbp/p300-interacting transactivator with glu/asp-rich C-terminal domain 1
9	0.832459	ILMN_226483	Bone γ-carboxyglutamate protein 2
10	0.828761	ILMN_218405	Expressed sequence ai451617
11	0.827349	ILMN_218425	Adenylate cyclase 2
12*	0.825594	ILMN_196778	IFN-induced transmembrane protein 1
13	0.821260	ILMN_209702	Glycine receptor, β-subunit
14	0.821191	ILMN_186983	
15*	0.818360	ILMN_185224	Dexh (Asp-Glu-X-His) box polypeptide 58
16*	0.818252	ILMN_185344	Proteasome (prosome, macropain) subunit, β-type 8
17	0.816414	ILMN_217565	Predicted gene 6907; predicted gene 6904; predicted gene 4902
18	0.815229	ILMN_225841	Solute carrier family 7, member 11
19	0.812510	ILMN_194594	
20*	0.811365	ILMN_214979	IFN-induced protein with tetratricopeptide repeats 3
21*	0.809468	ILMN_214321	Dexh (Asp-Glu-X-His) box polypeptide 58
22*	0.805007	ILMN_196777	IFN-induced transmembrane protein 3
23	0.804268	ILMN_218436	DNA damage-inducible transcript 4-like
24	0.803234	ILMN_211852	Purinergic receptor p2x, ligand-gated ion channel 4
25	0.801671	ILMN_218343	
26	0.797409	ILMN_193070	
27	0.795983	ILMN_214590	GST, pi 2; GST, pi 1
28	0.795591	ILMN_219340	Glutamate-cysteine ligase, modifier subunit
29	0.792238	ILMN_220932	
30*	0.790793	ILMN_196750	Histocompatibility 2, t-region locus 23
31*	0.785869	ILMN_210061	Phospholipase c, γ2
32*	0.783091	ILMN_253583	Chemokine (C-X-C motif) ligand 10 (IFN-γ–induced protein CRG-2)
33	0.782865	ILMN_213914	Angiopoietin 2
34	0.782641	ILMN_220401	
35	0.780631	ILMN_201755	
36	0.780488	ILMN_196409	
37*	0.779627	ILMN_257425	Dexh (Asp-Glu-X-His) box polypeptide 58
38	0.775060	ILMN_215955	G2 s phase-expressed protein 1
39	0.773665	ILMN_256110	Adenosine deaminase, rna-specific
40*	0.769889	ILMN_209202	IFN-γ–induced GTPase
41*	0.769203	ILMN_186258	Ubiquitin-specific peptidase 18
42	0.769026	ILMN_187187	Tripartite motif-containing 56
43	0.768357	ILMN_222570	Riken cdna 2310016c08 gene
44*	0.767755	ILMN_216138	Myxovirus (influenza virus) resistance 2
45*	0.765728	ILMN_196752	Histocompatibility 2, q-region locus 5
46	0.765117	ILMN_238157	Death inducer-obliterator 1
47	0.765001	ILMN_216376	Integral membrane protein 2b
48*	0.763112	ILMN_223999	Chemokine (c-x-c motif) ligand 10
49	0.762391	ILMN_211080	Thymocyte nuclear protein 1
50	0.762041	ILMN_213913	Atp synthase, h+ transporting, mitochondrial f0 complex, subunit s
51*	0.760474	ILMN_237558	Ww domain containing e3 ubiquitin protein ligase 1
52	0.758913	ILMN_215880	Proline-rich polypeptide 6
53	0.755828	ILMN_213057	MAPK kinase kinase kinase 1
54*	0.755805	ILMN_218776	Guanylate binding protein 6
55*	0.755243	ILMN_215351	ATPase, h+ transporting, lysosomal v0 subunit a1
56*	0.754930	ILMN_212179	2′-5′ oligoadenylate synthetase 1g
57	0.754898	ILMN_237580	High-mobility group box transcription factor 1
58	0.754254	ILMN_223985	
59*	0.753283	ILMN_211229	IRF7
60*	0.752297	ILMN_219577	Sequestosome 1
61	0.751231	ILMN_223944	Family with sequence similarity 70, member A
62	0.750676	ILMN_202718	Similar to unknown (protein for IMAGE: 4910858); predicted gene 4076
63*	0.748676	ILMN_212338	IFN-induced protein 35

Table S1. Cont.

Serial no.	Fracmaxamp	Illumina identification	Gene name
64	0.747622	ILMN_213017	Caveolin, caveolae protein 1
65	0.746548	ILMN_215799	
66*	0.746115	ILMN_217537	Inhibitor of DNA binding 2
67	0.745492	ILMN_214397	Coiled-coil domain containing 84
68*	0.743316	ILMN_214605	Radical s-adenosyl methionine domain containing 2
69	0.742414	ILMN_212540	Lysophosphatidylcholine acyltransferase 2
70	0.742413	ILMN_212110	Apolipoprotein L 9b; apolipoprotein L 9a
71	0.741198	ILMN_230539	Transient receptor potential cation channel, subfamily m, member 1
72	0.740058	ILMN_220818	Phosphoglycolate phosphatise
73	0.739570	ILMN_188510	
74	0.737070	ILMN_217201	Ectodermal-neural cortex 1
75	0.736869	ILMN_222986	Synaptophysin-like protein
76	0.735042	ILMN_210108	Heat-responsive protein 12
77	0.734609	ILMN_217932	Acyl-coa dehydrogenase, long-chain
78*	0.734464	ILMN_219674	Lipocalin 2
79*	0.733974	ILMN_223721	Guanine nucleotide binding protein (g protein), γ7 subunit
80	0.733795	ILMN_189853	Similar to tripartite motif protein TRIM34-α; tripartite motif-containing
81	0.732014	ILMN_213064	
82	0.731980	ILMN_213156	Rap guanine nucleotide exchange factor (gef) 4
83	0.731704	ILMN_203309	Riken cdna 1200016e24 gene
84	0.729582	ILMN_209247	Eukaryotic translation initiation factor 4e member 2
85*	0.729061	ILMN_209850	IRF1
86	0.728772	ILMN_192852	Ankyrin repeat and FYVE domain containing 1
87	0.728001	ILMN_218499	
88	0.725636	ILMN_220043	Proteolipid protein (myelin) 1
89	0.725446	ILMN_241583	Aldehyde dehydrogenase 4 family, member a1
90	0.725223	ILMN_221196	
91	0.724528	ILMN_203650	Unc-5 homolog c (*Caenorhabditis elegans*)
92	0.723849	ILMN_191462	
93	0.721978	ILMN_210363	
94	0.721533	ILMN_185693	
95	0.720974	ILMN_234373	Riken cdna 1810048j11 gene
96*	0.720583	ILMN_209781	2′-5′ oligoadenylate synthetase-like 2
97	0.720318	ILMN_221506	Bernardinelli-seip congenital lipodystrophy 2 homolog (human)
98	0.719436	ILMN_220771	Testis-expressed gene 2
99	0.719395	ILMN_196495	
100	0.718500	ILMN_186712	Unc-84 homolog a (*C. elegans*)
101*	0.718117	ILMN_193206	Ubiquitin-conjugating enzyme e2n
102	0.717922	ILMN_211574	Importin 13
103	0.717859	ILMN_202582	Stt3, subunit of the oligosaccharyltransferase complex
104	0.717748	ILMN_224259	Formin homology 2 domain containing 1
105	0.715915	ILMN_194391	Transformation-related protein 53-inducible nuclear protein 1
106	0.715812	ILMN_188004	
107*	0.715777	ILMN_192153	TNF receptor-associated factor 2
108	0.715619	ILMN_192099	
109	0.713326	ILMN_216296	Hemicentin 2
110	0.713066	ILMN_190871	Hexokinase 1
111	0.713043	ILMN_220667	Stt3, subunit of the oligosaccharyltransferase complex
112	0.712526	ILMN_210607	Guanine nucleotide binding protein (g protein), β-polypeptide 1-like
113*	0.711394	ILMN_210436	Guanylate nucleotide binding protein 2
114	0.710531	ILMN_208910	Family with sequence similarity 122, member B
115	0.709855	ILMN_215138	Budding uninhibited by benzimidazoles 3 homolog (*Saccharomyces cerevisiae*)
116	0.709693	ILMN_197368	
117	0.709485	ILMN_220503	Plasminogen activator, tissue
118	0.709362	ILMN_215301	Signal transducer and activator of transcription 2
119	0.709157	ILMN_194133	Tetratricopeptide repeat domain 7b
120	0.708279	ILMN_210695	Cdp-diacylglycerol-inositol 3-phosphatidyltransferase
121	0.707780	ILMN_211037	Oligophrenin 1
122	0.705834	ILMN_202025	Poly (ADP ribose) polymerase family, member 14
123	0.705386	ILMN_212511	Eukaryotic translation elongation factor 1 β2
124	0.704807	ILMN_190833	Inositol 1,4,5-triphosphate receptor interacting protein-like 1
125	0.704760	ILMN_220963	Formin-like 2

Table S1. Cont.

Serial no.	Fracmaxamp	Illumina identification	Gene name
126	0.704545	ILMN_229747	Basic leucine zipper transcription factor, ATF-like 3
127*	0.704483	ILMN_185655	Dual-specificity tyrosine-(Y)-phosphorylation–regulated kinase 3
128	0.704205	ILMN_184842	Mitochondrial ribosomal protein s10
129	0.703600	ILMN_187349	
130	0.702238	ILMN_233734	Carbonic anyhydrase 12
131	0.702040	ILMN_191331	
132*	0.701812	ILMN_221143	Hla-b–associated transcript 5
133	0.701722	ILMN_210247	ρ-GTPase activating protein 12
134	0.701543	ILMN_193808	
135	0.701461	ILMN_213966	Solute carrier family 44, member 3
136	0.701399	ILMN_217326	Coatomer protein complex subunit-α
137	0.701355	ILMN_189204	
138	0.701050	ILMN_224086	Rwd domain containing 2
139	0.700743	ILMN_211093	Nuclear factor of activated T cells 5
140	0.700695	ILMN_239612	Poly (ADP ribose) polymerase family, member 14
141	0.700107	ILMN_224541	Synaptotagmin-like 2

*Genes regulated by IFN-γ.